Acta Crystallographica Section F
Structural Biology and Crystallization Communications
ISSN 1744-3091

Crystallization and preliminary X-ray diffraction analysis of a high-affinity phosphate-binding protein endowed with phosphatase activity from *Pseudomonas aeruginosa* PAO1

Ahmed Djeghader,[a]‡ Guillaume Gotthard,[a]‡ Andrew Suh,[b] Daniel Gonzalez,[a] Ken Scott,[b] Eric Chabriere[a]* and Mikael Elias[c]*

[a]Aix Marseille Université, URMITE, UM63, CNRS 7278, IRD 198, Inserm 1095, 27 Boulevard Jean Moulin, 13385 Marseille CEDEX 5, France, [b]School of Biological Sciences, University of Auckland, Auckland, New Zealand, and [c]Biological Chemistry, Weizman Institute of Science, Rehovot, Israel

‡ These authors made equal contributions.

Correspondence e-mail: eric.chabriere@univmed.fr, mikael.elias@weizmann.ac.il

Received 10 July 2013
Accepted 28 August 2013

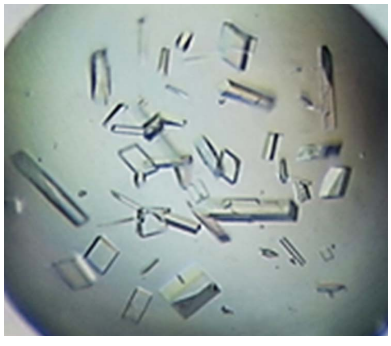

In prokaryotes, phosphate starvation induces the expression of numerous phosphate-responsive genes, such as the *pst* operon including the high-affinity phosphate-binding protein (PBP or pstS) and alkaline phosphatases such as PhoA. This response increases the cellular inorganic phosphate import efficiency. Notably, some *Pseudomonas* species secrete, *via* a type-2 secretion system, a phosphate-binding protein dubbed LapA endowed with phosphatase activity. Here, the expression, purification, crystallization and X-ray data collection at 0.87 Å resolution of LapA are described. Combined with biochemical and enzymatic characterization, the structure of this intriguing phosphate-binding protein will help to elucidate the molecular origin of its phosphatase activity and to decipher its putative role in phosphate uptake.

1. Introduction

Phosphorus is an essential nutrient for all living cells as it is a key component of biomolecules such as DNA. However, although phosphate (P_i) is relatively abundant on Earth, its bioavailability is limited (Cordell & White, 2011). Bacteria therefore possess different tools for cellular phosphate uptake (Wanner, 1993), such as the Pit (phosphate inorganic transport) system that is usually used and expressed when P_i is plentiful (Willsky & Malamy, 1980). On the other hand, under P_i limitation conditions or in the presence of high concentrations of competing anions, the PhoB–PhoR two-component system which senses variation of P_i concentration in the environment induces the transcription of numerous genes related to P_i assimilation (Hsieh & Wanner, 2010). The phosphate-specific transport (Pst) system is highly expressed under such conditions, including the high-affinity extracellular (or periplasmic) phosphate-binding protein (called PstS or PBP), in order to scavenge the phosphate present in the environment (Willsky & Malamy, 1980; Wanner, 1993; Elias *et al.*, 2012). Phosphate starvation also induces the expression of a large variety of genes that enable the extraction of phosphate from sources other than P_i, such as organophosphate compounds (Dyhrman *et al.*, 2006). A well documented example is alkaline phosphatases such as PhoA (Ohtake *et al.*, 1998; VanBogelen *et al.*, 1996).

Alkaline phosphatases (EC 3.1.3.1) are nonspecific esterases that catalyze phosphate monoester hydrolysis *via* a phosphoseryl intermediate to yield P_i and an alcohol (Coleman, 1992; Sun *et al.*, 1999). They thus hydrolyze non-transportable organophosphate compounds to release P_i that may be subsequently taken up by the Pit or Pst systems (Wanner, 1993). Homologous proteins to PhoA exist in many bacterial species, including *Pseudomonas* (Kriakov *et al.*, 2003; Filloux *et al.*, 1988). Interestingly, in addition to PstS and PhoA, some *Pseudomonas* species possess phosphate-binding proteins (PBPs) endowed with phosphatase activity. Indeed, one of these proteins, dubbed low-molecular-weight alkaline phosphatase (LapA), is able to hydrolyze *para*-nitrophenyl phosphate (pNPP; specific activity 46 U mg^{-1}, where 1 U mg^{-1} represents one micromole of pNPP hydrolyzed per minute per milligram of protein; Tan & Worobec, 1993). In contrast to PhoA, which is constitutively produced by *P. aeruginosa* PAO1, LapA expression is induced solely under P_i limitation (Tan & Worobec, 1993; Ball *et al.*, 2002).

LapA-like proteins belong to the PBP superfamily and seem to form a specific clade (Fig. 1). The LapA-encoding gene displays a

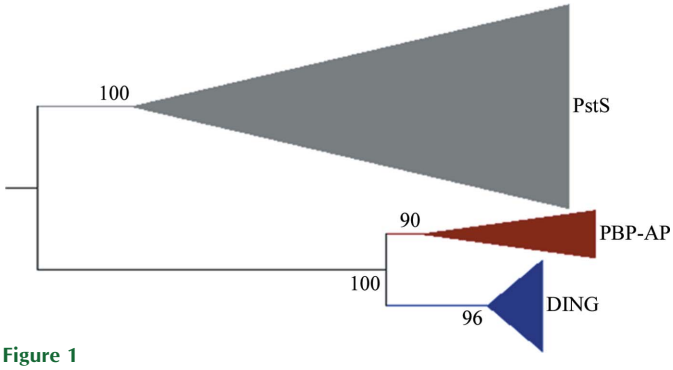

Figure 1
Collapsed phylogenetic tree of the phosphate-binding protein superfamily. PBP-AP represents the family of phosphate-binding proteins endowed with phosphatase activity. The sequences were collected from the NCBI database using the LapA sequence as the query. A total of 153 sequences were subsequently aligned using the *MUSCLE* program (Edgar, 2004). The phylogenetic tree was built using the *MEGA* software (Tamura *et al.*, 2011). Bootstrap values are shown for each node of the tree.

similar genetic organization to that observed for a clade of the PBP superfamily: DING proteins, which are also induced by phosphate starvation (Liebschner *et al.*, 2009; Zhang *et al.*, 2007). These genes locate between an Hxc type-2 secretion system (T2SS) and a haemagglutinin-like protein (Zhang *et al.*, 2007; Djeghader *et al.*, 2013). This specific localization downstream from the T2SS allows the secretion of these proteins by this machinery. Interestingly, this T2SS seems to be dedicated to the unique secretion of LapA-like proteins and DING proteins (Ball *et al.*, 2012; Douzi *et al.*, 2012; Filloux, 2011).

The isolation of PBPs that exhibit phosphatase activity is intriguing, since high-affinity PBPs and alkaline phosphatase are both overexpressed during phosphate starvation. Proteins such as LapA might thus have a unique, as yet unexplored role in phosphate starvation. The determination of its structure, coupled with careful biochemical and functional characterization, will be of great value in deciphering the role of these proteins in phosphate uptake in *Pseudomonas*. Here, we report the crystallization, data collection at 0.87 Å resolution and preliminary crystallographic analysis of LapA.

2. Methods and materials

2.1. Cloning, expression and purification of LapA protein

The LapA-encoding gene was amplified from *P. aeruginosa* PAO1 genomic DNA (accession No. NC_002516; locus tag PA0688) using the same strategy as used for the amplification of the PA14DING gene (Djeghader *et al.*, 2013). Briefly, primers LapAF, 5′-GGC AGC GGC GCG GTC ACC GGC GGT GGC GCT T-3′, and LapAR, 5′-GAA AGC TGG GTG TTA CGG GCG GCC TTT GGT G-3′, were designed according to the *lapA* sequence and used for an initial amplification. Using the obtained product, a second PCR step was performed using primers containing the *att*B1 and *att*B2 Gateway recombination sites (GatewayF, 5′-GGGG ACA AGT TTG TAC AAA AAA GCA GGC TTC GAA AAC CTG TAT TTT CAG GGC AGC GGC GCG-3′; GatewayR, 5′-GGGG AC CAC TTT GTA CAA GAA AGC TGG GTG-3′) which allow cloning into the Gateway pDONR221 vector (Moreland *et al.*, 2005). Downstream of the GatewayF primer, a *Tobacco etch virus* (TEV) protease recognition site was added to allow removal of the fusion tag. Finally, the *lapA* gene was cloned into the destination vector pDEST-periHisMBP (Addgene plasmid 11086; Nallamsetty *et al.*, 2005), allowing the expression of an N-terminal hexa-His-MBP tag for affinity purification of the protein. The resulting vector was transformed into *Escherichia coli* DH5*α* and extracted using the QIAprep Spin Miniprep Kit (Qiagen). The identity of the cloned gene was verified by sequencing.

The fusion protein (His-MBP-LapA) was overexpressed in *E. coli* BL21(DE3)-pLysS strain (see construct sequence in Fig. 2*a*). As in the cases of homologues of LapA, the periplasmic expression of the protein did not require the use of periplasmic extraction protocols (Ahn *et al.*, 2007; Moniot *et al.*, 2007; Djeghader *et al.*, 2013). Protein expression was performed overnight at 310 K in 4 l auto-inducible ZYP medium (Studier, 2005) inoculated with 100 ml overnight preculture in the presence of 100 µg ml^{-1} ampicillin and 34 µg ml^{-1} chloramphenicol. Cells were then harvested by centrifugation (5000*g*, 15 min, 277 K), resuspended in lysis buffer (300 m*M* NaCl, 10 m*M* imidazole, 50 m*M* Tris pH 8, 1 m*M* PMSF, 0.25 mg ml^{-1} lysozyme, 10 µg ml^{-1} DNAse I, 20 m*M* $MgSO_4$) and stored at 193 K for 2 h.

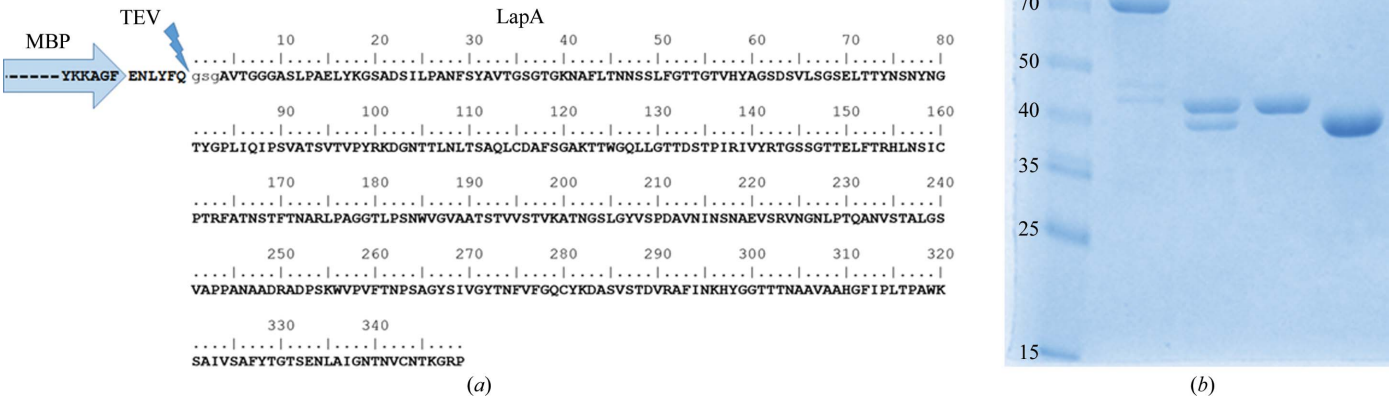

Figure 2
(*a*) View of the expressed construct. It encodes the sequence of the MBP (in blue), the TEV protease cleavage site and the protein sequence (LapA). The three residues from the expression tag that remain on LapA after TEV cleavage are shown in lower case. (*b*) 12% SDS–PAGE related to purification steps of LapA. Lane MWM, molecular-weight markers (Thermo Scientific Spectra Multicolor Broad Range Protein Ladder; labelled in kDa); lane 1, His-MBP-LapA fusion protein; lane 2, TEV protease-cleavage products; lanes 3 and 4, MBP and LapA (5 µg), respectively, separated by the anion-exchange column.

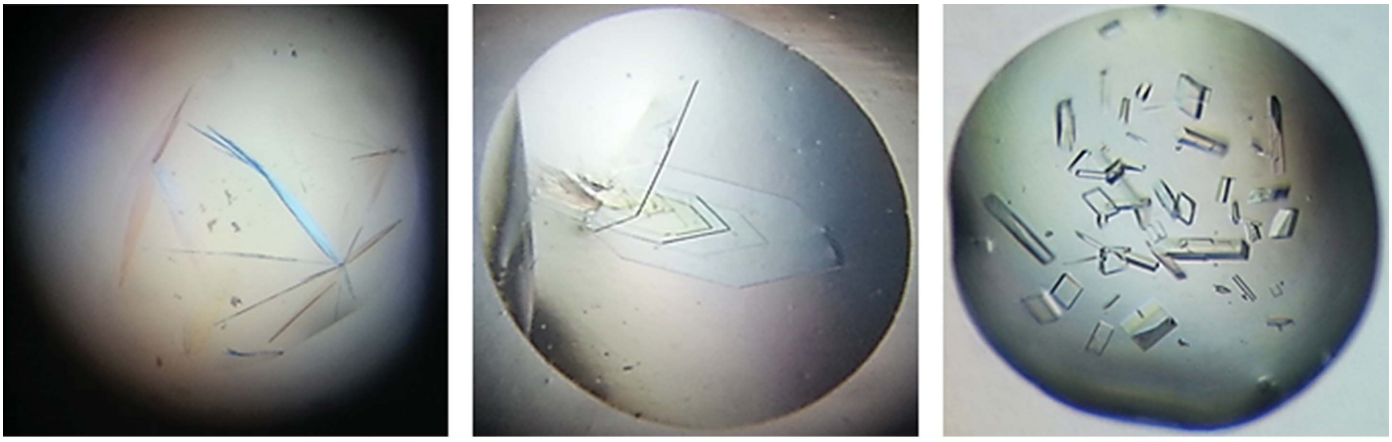

(*a*) (*b*) (*c*)

Figure 3
Evolution of LapA crystals during crystallization. (*a*) Needles from the Wizard I and II screen, (*b*) crystal plates obtained from the optimized conditions, (*c*) LapA crystals improved by re-screening and microseeding.

After thawing, complete lysis of the cells was achieved by sonication (Vibracell 75185; 30 s, 80% intensity). Cell debris was then pelleted by centrifugation (17 000*g*, 30 min, 277 K) and the supernatant was loaded onto a nickel-affinity column (HisTrap FF crude, GE Healthcare) at a flow rate of 5 ml min^{-1}. Elution of His-MBP-LapA protein was performed using a buffer consisting of 300 m*M* NaCl, 500 m*M* imidazole, 50 m*M* Tris pH 8. Eluted proteins were then applied onto a size-exclusion chromatography column (Superdex 75 16/60, GE Healthcare) in 20 m*M* NaCl, 20 m*M* Tris pH 8 buffer to eliminate contaminant proteins. Fractions containing the fusion protein (Fig. 2*b*, lane 1) were pooled and incubated with 1.25 mg TEV protease overnight at 289 K in the presence of 0.5 m*M* EDTA and 1 m*M* DTT. The two proteins resulting from TEV protease cleavage migrated with almost the same mobility (around 40 kDa as observed on 12% SDS–PAGE; Fig. 2*b*, lane 2). Taking advantage of their different isoelectric points (pI 5.0 for MBP and 8.98 for LapA), it was possible to separate them on an anion-exchange column (Resource Q, GE Healthcare; Fig. 2*b*, lanes 3 and 4). Finally, pure LapA was recovered, concentrated to 12.5 mg ml^{-1} (Amicon Ultra MWCO 10 kDa; Millipore, Ireland) and used for crystallization assays.

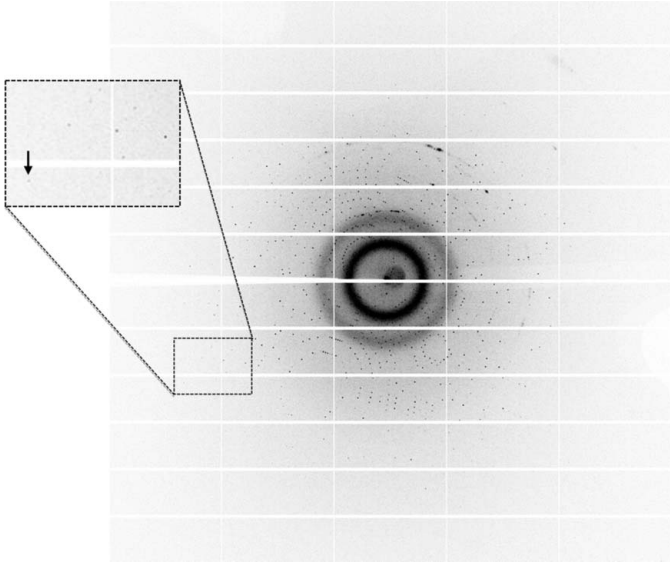

Figure 4
A diffraction pattern from a LapA crystal. The edge of the frame is at 0.8 Å resolution. The spot indicated by the arrow is at 0.86 Å.

2.2. Protein crystallization

Crystallization assays were performed in 96-well trays using the sitting-drop vapour-diffusion method implemented on a nanodrop dispensing robot (Mosquito, TTP Labtech) and incubated at 298 K. Initial screening (192 drops of 750 nl, with protein:crystallization solution ratios of 2:1 and 1:1) was performed using the commercial crystallization screens Wizard I and II (Emerald BioSystems). Needles and clusters appeared in several conditions in a few hours, and the best hit was identified in a condition consisting of 30%(*v*/*v*) PEG 8000, 200 m*M* Li_2SO_4, 100 m*M* sodium acetate/acetic acid pH 4.5 (Fig. 3*a*). This condition was optimized for pH (4.0–5.5) and PEG concentration (15–30%) using the hanging-drop method (64 drops), but only thin plates appeared after 1–2 h in different conditions (Fig. 3*b*). To overcome this issue, a microseeding strategy was undertaken. An initial strategy consisted of crushing a crystal and diluting it in 100 µl crystallization solution (20% PEG 8000, 200 m*M* Li_2SO_4, 100 m*M* sodium acetate/acetic acid pH 4.75). The drops were subsequently inoculated with 25 nl of this seeding solution. However, this strategy did not improve the crystal quality. The same strategy was repeated but adding 10% of the initial commercial screen solution as an additive to the crystallization solution and by using the seeding solution at 1:1000 dilution. Diffraction-quality crystals appeared after 2 d (Fig. 3*c*). The final condition consisted of 20% PEG 8000, 250 m*M* NaCl, 200 m*M* Li_2SO_4, 100 m*M* sodium acetate/acetic acid pH 4.75.

2.3. Data collection

The crystals for the diffraction experiment were cryoprotected using a solution consisting of the crystallization solution containing 20%(*v*/*v*) glycerol prior to mounting on a MicroLoop (MiTeGen) and flash-cooling in liquid nitrogen. X-ray diffraction intensities were collected on the ID23-1 beamline at the European Synchrotron Radiation Facility (ESRF, Grenoble, France) using a wavelength of 0.799 Å and a PILATUS 6M detector with 37 ms exposure. A total of 3600 images were collected using the fine-slicing method and the

Table 1
Data-collection statistics.

Values in parentheses are for the last bin.

Beamline	ID-23-1
Wavelength (Å)	0.799
Detector	PILATUS 6M
Oscillation (°)	0.1
No. of frames	2000
Resolution (Å)	0.87 (0.95–0.87)
Space group	$P2_1$
Unit-cell parameters (Å, °)	a = 40.76, b = 67.63, c = 57.62, β = 110.4
No. of observed reflections	830383 (177520)
No. of unique reflections	231568 (52382)
Completeness (%)	96.8 (94.7)
R_{meas}† (%)	5.3 (42.8)
R_{merge} (%)	4.5 (36.1)
$CC_{1/2}$	99.9 (87.3)
$\langle I/\sigma(I)\rangle$‡	15.25 (3.47)
Multiplicity	3.59 (3.39)
Mosaicity (°)	0.184

† The redundancy-independent merging R factor $R_{meas} = \sum_{hkl}\{N(hkl)/[N(hkl)-1]\}^{1/2}\sum_i |I_i(hkl) - \langle I(hkl)\rangle|/\sum_{hkl}\sum_i I_i(hkl)$. ‡ $I/\sigma(I)$ is the signal-to-noise ratio.

individual frames consisted of 0.1° steps over a range of 360° (Fig. 4). Among these images, 2000 were retained for data integration and scaling to minimize the effect of radiation decay.

3. Results and conclusions

Integration and scaling of X-ray diffraction data were performed using *XDS* (Kabsch, 2010; Table 1). The LapA crystal belonged to the monoclinic space group $P2_1$, with unit-cell parameters a = 40.76, b = 67.63, c = 57.62 Å, β = 110.4°. Molecular replacement was performed with *Phaser* (McCoy *et al.*, 2007) using the structure of *Pseudomonas fluorescens* DING as a model (44% sequence identity to LapA; PDB entry 2q9t; Ahn *et al.*, 2007), in which regions corresponding to protruding loops in the structure were deleted from the PDB model file (residues 217–221, 239–246 and 279–287). One molecule was placed per asymmetric unit (R_{free} = 30.38%) as suggested by the calculated Matthews coefficient (2.07 $Å^3\,Da^{-1}$ corresponding to 40.50% solvent content; Matthews, 1968) and the crystal packing was clearly complete. Manual model improvement was performed using *Coot* (Emsley *et al.*, 2010) and refinement was performed using *REFMAC* (Murshudov *et al.*, 2011). The current R_{free} is 12.40%. The construction, refinement and interpretation of the sub-Å resolution structure of LapA are in progress.

AD is a PhD student supported by Aix-Marseille Université. GG is a PhD student/AP-HM engineer in charge of the protein purification/crystallization platform. DG is a PhD student/AP-HM engineer. AS and KS thank the Auckland Medical Research Foundation and the University of Auckland for support.

References

Ahn, S., Moniot, S., Elias, M., Chabriere, E., Kim, D. & Scott, K. (2007). *FEBS Lett.* **581**, 3455–3460.
Ball, G., Durand, E., Lazdunski, A. & Filloux, A. (2002). *Mol. Microbiol.* **43**, 475–485.
Ball, G., Viarre, V., Garvis, S., Voulhoux, R. & Filloux, A. (2012). *Res. Microbiol.* **163**, 457–469.
Coleman, J. E. (1992). *Annu. Rev. Biophys. Biomol. Struct.* **21**, 441–483.
Cordell, D. & White, S. (2011). *Sustainability*, **3**, 2027–2049.
Djeghader, A., Gotthard, G., Suh, A., Gonzalez, D., Scott, K., Elias, M. & Chabriere, E. (2013). *Acta Cryst.* F**69**, 425–429.
Douzi, B., Filloux, A. & Voulhoux, R. (2012). *Philos. Trans. R. Soc. Lond. B Biol. Sci.* **367**, 1059–1072.
Dyhrman, S. T., Chappell, P. D., Haley, S. T., Moffett, J. W., Orchard, E. D., Waterbury, J. B. & Webb, E. A. (2006). *Nature (London)*, **439**, 68–71.
Edgar, R. C. (2004). *Nucleic Acids Res.* **32**, 1792–1797.
Elias, M., Wellner, A., Goldin-Azulay, K., Chabriere, E., Vorholt, J. A., Erb, T. J. & Tawfik, D. S. (2012). *Nature (London)*, **491**, 134–137.
Emsley, P., Lohkamp, B., Scott, W. G. & Cowtan, K. (2010). *Acta Cryst.* D**66**, 486–501.
Filloux, A. (2011). *Front. Microbiol.* **2**, 155.
Filloux, A., Bally, M., Soscia, C., Murgier, M. & Lazdunski, A. (1988). *Mol. Gen. Genet.* **212**, 510–513.
Hsieh, Y.-J. & Wanner, B. L. (2010). *Curr. Opin. Microbiol.* **13**, 198–203.
Kabsch, W. (2010). *Acta Cryst.* D**66**, 125–132.
Kriakov, J., Lee, S. & Jacobs, W. R. Jr (2003). *J. Bacteriol.* **185**, 4983–4991.
Liebschner, D., Elias, M., Moniot, S., Fournier, B., Scott, K., Jelsch, C., Guillot, B., Lecomte, C. & Chabrière, E. (2009). *J. Am. Chem. Soc.* **131**, 7879–7886.
Matthews, B. W. (1968). *J. Mol. Biol.* **33**, 491–497.
McCoy, A. J., Grosse-Kunstleve, R. W., Adams, P. D., Winn, M. D., Storoni, L. C. & Read, R. J. (2007). *J. Appl. Cryst.* **40**, 658–674.
Moniot, S., Elias, M., Kim, D., Scott, K. & Chabriere, E. (2007). *Acta Cryst.* F**63**, 590–592.
Moreland, N., Ashton, R., Baker, H. M., Ivanovic, I., Patterson, S., Arcus, V. L., Baker, E. N. & Lott, J. S. (2005). *Acta Cryst.* D**61**, 1378–1385.
Murshudov, G. N., Skubák, P., Lebedev, A. A., Pannu, N. S., Steiner, R. A., Nicholls, R. A., Winn, M. D., Long, F. & Vagin, A. A. (2011). *Acta Cryst.* D**67**, 355–367.
Nallamsetty, S., Austin, B. P., Penrose, K. J. & Waugh, D. S. (2005). *Protein Sci.* **14**, 2964–2971.
Ohtake, H., Kato, J., Kuroda, A., Wu, H. & Ikeda, T. (1998). *J. Biosci.* **23**, 491–499.
Studier, F. W. (2005). *Protein Expr. Purif.* **41**, 207–234.
Sun, L., Martin, D. C. & Kantrowitz, E. R. (1999). *Biochemistry*, **38**, 2842–2848.
Tamura, K., Peterson, D., Peterson, N., Stecher, G., Nei, M. & Kumar, S. (2011). *Mol. Biol. Evol.* **28**, 2731–2739.
Tan, A. S. P. & Worobec, E. A. (1993). *FEMS Microbiol. Lett.* **106**, 281–286.
VanBogelen, R. A., Olson, E. R., Wanner, B. L. & Neidhardt, F. C. (1996). *J. Bacteriol.* **178**, 4344–4366.
Wanner, B. L. (1993). *J. Cell. Biochem.* **51**, 47–54.
Willsky, G. R. & Malamy, M. H. (1980). *J. Bacteriol.* **144**, 356–365.
Zhang, X.-X., Scott, K., Meffin, R. & Rainey, P. B. (2007). *BMC Microbiol.* **7**, 114.